metals

MDPI

Article

Effect of Cr_2O_3 on Physicochemical Properties of CaO-SiO_2-Fe_tO Slags during BOF Smelting Process of Chromium-Bearing Iron

Shannan Li [1], Jianli Li [1,2,3,*], Yue Yu [1,2] and Hangyu Zhu [1,3]

[1] The State Key Laboratory of Refractories and Metallurgy, Wuhan University of Science and Technology, Wuhan 430081, China; lsn98@wust.edu.cn (S.L.); yuyue@wust.edu.cn (Y.Y.); zhuhy@wust.edu.cn (H.Z.)
[2] Hubei Provincial Key Laboratory for New Processes of Ironmaking and Steelmaking, Wuhan University of Science and Technology, Wuhan 430081, China
[3] Key Laboratory for Ferrous Metallurgy and Resources Utilization of Ministry of Education, Wuhan University of Science and Technology, Wuhan 430081, China
* Correspondence: jli@wust.edu.cn

Abstract: The productivity of basic-oxygen-furnace (BOF) smelting process is directly affected by the slag-forming speed during the initial stage of converter. Therefore, it is essential to study the effect of different Cr_2O_3 content on the physicochemical properties of the primary slag in the smelting process of chromium-bearing semi-steel. In this work, Factsage8.1 software, X-ray diffraction (XRD), scanning electron microscope (SEM), energy dispersive spectroscopy (EDS) and a high-temperature melting point tester were used to study the effects of different Cr_2O_3 content on the melting temperature, solidification behavior, mineral composition, and other physicochemical properties of the CaO-SiO_2-Fe_tO system. The results showed that the melting temperature of slag samples increased from 1223 °C to 1354 °C as Cr_2O_3 increased from 0 wt% to 9.09 wt%. With the increase of Cr_2O_3, the content of $CaFeSi_2O_6$ decreased. Moreover, due to the addition of Cr_2O_3, the chromium-bearing spinel solid solution ($Fe(Fe,Cr)_2O_4$) began to form in the slag. Furthermore, Cr_2O_3 promoted the increase in the volume of free solid particles in the slag, resulting in an increase in slag viscosity. All in all, the increase of Cr_2O_3 content in the CaO-SiO_2-Fe_tO system will adversely affect the semi-steel steelmaking process.

Keywords: Cr_2O_3; vanadium–titanium magnetite; slag; mineral composition; spinel

Citation: Li, S.; Li, J.; Yu, Y.; Zhu, H. Effect of Cr_2O_3 on Physicochemical Properties of CaO-SiO_2-Fe_tO Slags during BOF Smelting Process of Chromium-Bearing Iron. *Metals* **2022**, *12*, 1110. https://doi.org/10.3390/met12071110

Academic Editor: Alexander Ivanovich Zaitsev

Received: 10 May 2022
Accepted: 25 June 2022
Published: 28 June 2022

1. Introduction

High-chromium vanadium–titanium magnetite (HCVT) is a typical multimetal cooccurring mineral resource, which has iron, titanium, vanadium, chromium, and other resources [1,2]. HCVT is mainly utilized through the blast furnace process [3], and molten iron is smelted by the converter to obtain semi-steel. However, the semi-steel obtained by the vanadium extraction converter process contains chromium [4]. In the steelmaking converter process, the rapid formation of a suitable and stable slag is conducive to the dissolution of lime to increase the basicity, which is beneficial to improve the dephosphorization reaction rate, reduce the amount of flux, purify molten steel, and improve productivity [4]. However, under the smelting conditions of the steelmaking converter, [Cr] in the semi-steel is oxidized to (Cr_2O_3) and enters the slag. The (Cr_2O_3) then reacts with (FeO) in the slag to form spinel. Cr_2O_3 and chromium-containing spinel phases have high melting points. The melting points of Cr_2O_3, $FeCr_2O_4$ and $MgCr_2O_4$ are 2435 °C, 2000 °C, and 2350 °C, respectively [5,6]. The high melting point phase in the slag is not conducive to the dissolution of lime. Therefore, Cr_2O_3 has a great influence on the production of converter.

$$2[Cr]+3(FeO) = (Cr_2O_3)+3[Fe] \quad (1)$$

$$(Cr_2O_3) + (FeO) = (FeCr_2O_4) \quad (2)$$

Several researchers have studied the influence of Cr_2O_3 content on the metallurgical properties of molten slag. Cheng [7] studied the effect of Cr_2O_3 on the reduction smelting mechanism of high chromium vanadium titanomagnetite pellets. It was found that the softening initiation temperature and softening temperature gradually increased as the content of Cr_2O_3 increased from 0.28% to 8.22%. In addition, the melting start temperature and the dripping temperature gradually increased. Qiu [8] found that the viscosity of the blast furnace slag in the 29.3% CaO-26.7% SiO_2-8% MgO-22% TiO_2-14% Al_2O_3 system increased significantly as the Cr_2O_3 content increased from 0% to 4%. Xu [9] added 1%, 3%, and 5% Cr_2O_3 to the mold slag used for casting high-carbon chromium steel (Cr12MoV). The results showed that with the increase of Cr_2O_3 content, both the melting temperature and viscosity increased. Babenko [5] reported the effect of Cr_2O_3 on the viscosity of AOD slag in the CaO-SiO_2-Cr_2O_3 system containing 8% MgO, 3% Al_2O_3, and 6% B_2O_3. Experiments showed that compared with the slag without Cr_2O_3, the slag containing 18% Cr_2O_3 had a higher temperature required to maintain sufficient fluidity (viscosity <1 Pa·s), and the temperature range was narrower. Li [10] studied CaO-SiO_2-MgO-Al_2O_3-Cr_2O_3 slag at 1550 °C. In silicate networks, the Cr^{3+} ions act as the network formers and increase the degree of polymerization (DOP). The viscosity of the slag increases with the increase of Cr_2O_3. Wu [11] studied the effect of Cr_2O_3 on the viscosity of CaO-SiO_2-10% Al_2O_3-Cr_2O_3 quaternary slag from 1540 °C to 1680 °C. With the increase of Cr_2O_3 content, the viscosity of the slags decreased at both basicities (R = 1.2 and R = 0.8), and the viscosity of the acidic slag decreased more. Xu [12] found that the viscosity of CaO-SiO_2-MgO-23.2% Al_2O_3-TiO_2 slag increased with the addition of Cr_2O_3, and the viscosity of the high Cr_2O_3-containing slag increased even more. Liu [13] reported the effect of the Cr_2O_3 content on the viscosity of stainless-steel-making slags. In a low basicity (R = 0.57) slag, increasing the Cr_2O_3 content resulted in a lower viscosity. In slag with high basicity (R = 1.54), an increased Cr_2O_3 content resulted in an increased viscosity.

However, there are few reports on the effect of Cr_2O_3 on the slag in the initial stage of the steelmaking converter. The content of [Si], [Mn], and [C] elements in semi-steel are low, and the heat generation is insufficient during the steelmaking process [14]. The high-melting-point chromium-containing phase will deteriorate the metallurgical properties of the slag. This work aims to study the effect of the Cr_2O_3 content addition on the melting temperature, solidification behavior, mineral composition, microstructure, and other physicochemical properties of the CaO-SiO_2-Fe_tO system according to thermodynamic analysis and lab experiments.

2. Materials and Methods

2.1. Raw Materials

Referring to the composition of the slag in the initial stage of the converter smelting process, the 19% CaO-42% SiO_2-39% Fe_tO system was selected as the basic slag A0. Then, 1 wt%, 3 wt%, 5 wt%, 7 wt% and 10 wt% of Cr_2O_3 were additionally added to A0, respectively. The mass percentages of slag composition are shown in Table 1. The experiment used analytical reagent powders CaO, SiO_2, Cr_2O_3, and $FeC_2O_4{\cdot}2H_2O$ produced by Sinopharm Group as raw materials, in which $FeC_2O_4{\cdot}2H_2O$ replaces FeO in the system. Each reagent was weighed according to the compositions in Table 1 and mixed evenly. The mixed reagents were sieved with 15-mesh and 35-mesh sieves 3 times to prepare the slag samples.

2.2. Preparing the Slag Samples

Iron(II) oxalate dihydrate ($FeC_2O_4{\cdot}2H_2O$) decomposes into H_2O, CO, and CO_2 gases at a temperature of about 300 °C. If the slag samples are heated directly to the melting

temperature, they may be sprayed on the furnace tube wall. In this work, the slag samples were first sintered to eliminate gas and reduce the volume. Each slag sample was charged in the corundum crucible (Φ 60 × 120 mm) and compacted, and then the crucibles were placed in the muffle furnace. High-purity nitrogen (99.999% N_2) was passed into the furnace at a flow rate of 0.5 L per minute. The muffle furnace was heated to 1100 °C at a heating rate of 5 °C per minute. After the slag samples were sintered for 30 min, they were cooled to room temperature in the furnace. The slag samples were charged into magnesium oxide crucibles (Φ 40 × 100 mm) and compacted. The crucible was placed in a 35 kW high-temperature carbon tube furnace. As the protective atmosphere, high-purity nitrogen was passed into the furnace at a flow rate of 0.5 L per minute. The furnace was heated to 1500 °C at a rate of 10 °C/min and held for 5 min to make the temperature and composition of the molten slag uniform. Then, the molten slag was extracted with a syringe and hollow quartz tube with a diameter of 4 mm, and the slag was cooled in air. Slag samples were stored in vacuum canisters for subsequent testing.

Table 1. Chemical composition of slag, wt%.

No.	CaO	SiO_2	FeO	Cr_2O_3
A0	19.00	42.00	39.00	0.00
A1	18.81	41.58	38.61	0.99
A2	18.45	40.78	37.86	2.91
A3	18.10	40.00	37.14	4.76
A4	17.76	39.25	36.45	6.54
A5	17.27	38.18	35.45	9.09

2.3. Methods

The slag samples A0 to A5 were each taken and put into the metallographic mounting machine (XQ-2B, BANGYES Precision Measuring Instrument (Shanghai) Co., Ltd., Shanghai, China) with the metallographic (hot) mounting resins resin (HMR4, Wuhan Sanling New Meterials Co.,Ltd, Wuhan, China). The temperature was raised to 160 °C and kept for 20 min. Then, the samples were removed and air-cooled. After the samples were polished, their surface was sprayed with gold. The microscopic morphology of the sample was observed using a scanning electron microscope (ASIN EVO10, Carl Zeiss AG, Oberkochen, Germany).

Each slag sample was ground to 325 mesh or more with a grinder to obtain a powder sample. Each powder sample was subjected to an X-ray diffraction (XPert PRO MPD, PANalytical B.V., Almelo, The Netherlands) analysis. The XRD test results were analyzed by MDI Jade (6, Materials Data, Livermore, CA, USA).

The melting temperature of slag samples A0–A5 was measured by the hemisphere point method. First, two grams of powder samples were taken out and mixed with an appropriate amount of saturated aqueous solution of corn dextrin. Then, the sample was pressed into a cylindrical sample of Φ 3 × 3 mm with a mold. The samples were placed in the high-temperature visualization resistance furnace (SYD-RW286, Anshan S.Y.D Science and Technology Co. Ltd., Anshan, China), and the furnace was heated at a rate of 10 °C/min. We used the accompanying software program to record changes in sample height.

3. Results

3.1. Effect of Different Cr_2O_3 Contents on the Melting Point of the Slags

The melting temperature of the slag sample is shown in Table 2. The samples are acidic slags and the basicity is 0.45. The melting temperature range of acidic slag is wide and there is no definite melting point. The temperature at which the height of the sample drops to three-quarters and one-half of the original height is referred to as the softening point temperature and the hemispherical point temperature, respectively. Generally, the hemispheric point temperature is used as the melting temperature of slag. It can be seen

from Table 2 that as $w(Cr_2O_3)$ in the CaO-SiO_2-Fe_tO system increases from 0 wt% to 9.09 wt%, the melting temperature of the slag increases from 1223 °C to 1354 °C. The fundamental reason for the increase of the melting temperature of the CaO-SiO_2-Fe_tO system is that the addition of Cr_2O_3 leads to the precipitation of the spinel solid solution in the slag [9].

Table 2. The relationship between melting temperature of synthetic slag and Cr_2O_3 content, °C.

No.	Softening Point	Hemisphere Point
A0	1183	1223
A1	1186	1193
A2	1195	1243
A3	1192	1257
A4	1213	1335
A5	1259	1354

3.2. Effect of Different Cr_2O_3 Contents on the Mineral phase of the Slag

As shown in Figure 1, the main phases in the system are calcium iron pyroxene ($CaFeSi_2O_6$) and spinel ($FeCr_2O_4$ and Fe_3O_4). The melting point of $CaFeSi_2O_6$ is 1150 °C, so it is in a liquid phase at 1500 °C. According to the XRD results, the spinel phase in sample A0 was iron spinel (Fe_3O_4), and the spinel phase in samples A1 to A5 was iron spinel and iron chromium spinel ($FeCr_2O_4$). In Figure 1, the peak at 29.8° is the main peak of $CaFeSi_2O_6$, and the peak at 35.5° is the main peak of $FeCr_2O_4$ and Fe_3O_4. With the increase of Cr_2O_3 content, the intensity of the 29.8° peak showed a weakening trend, while the intensity of 35.5° peak gradually increased. When the Cr_2O_3 content was 9.09 wt%, the 56° and 62.6° peaks of $FeCr_2O_4$ also became sharp. The intensity of the XRD peaks was positively correlated with the content of the crystalline phase. In summary, the liquid phase in the CaO-SiO_2-Fe_tO system gradually decreased with the increase of $w(Cr_2O_3)$, and the content of chromium-containing spinel gradually increased. This is discussed further in subsequent sections.

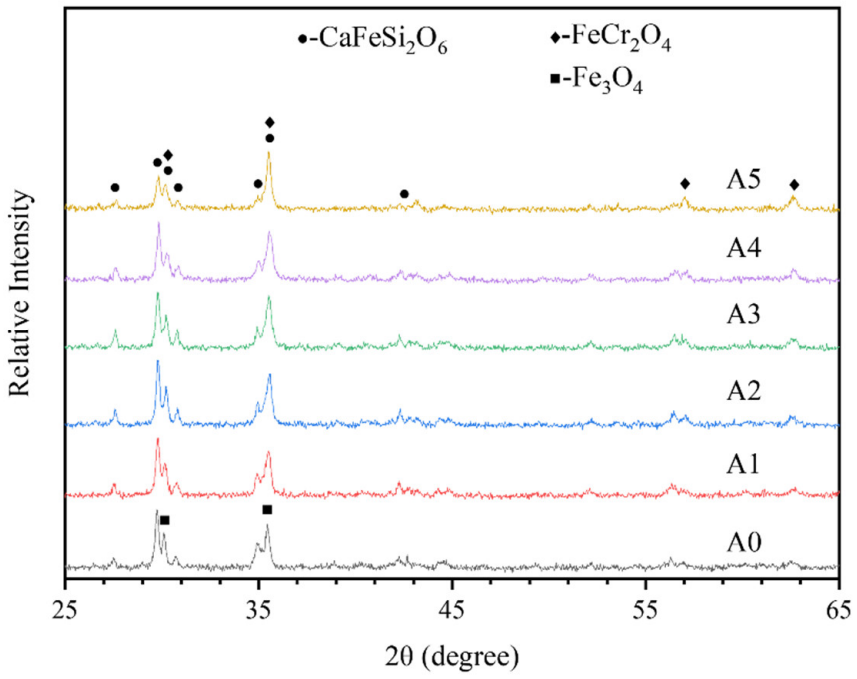

Figure 1. XRD analysis results of adding different Cr_2O_3 content to CaO-SiO_2-Fe_tO system.

3.3. Effect of Different Cr_2O_3 Contents on the Microstructure of the Slag

The SEM images of the high temperature samples of the CaO-SiO_2-Fe_tO system with different Cr_2O_3 content are shown in Figure 2, and samples A0 to A5 correspond to Figure 2a–f, respectively. There are three phases in the system, and their typical compositions are shown in Table 3. Phase 1 is calcium iron pyroxene ($CaFeSi_2O_6$), phase 2 is iron spinel (Fe_3O_4), and phase 3 is chromium-containing iron spinel ($Fe(Fe,Cr)_2O_4$). Calcium iron pyroxene is the basic liquid phase of the CaO-SiO_2-FetO system at 1500 °C. The elemental composition of the chain-like white particles in Figure 2a–d is shown in no. IV in Table 3. The authors believe that they are spinel particles precipitated in the late stage of slag solidification.

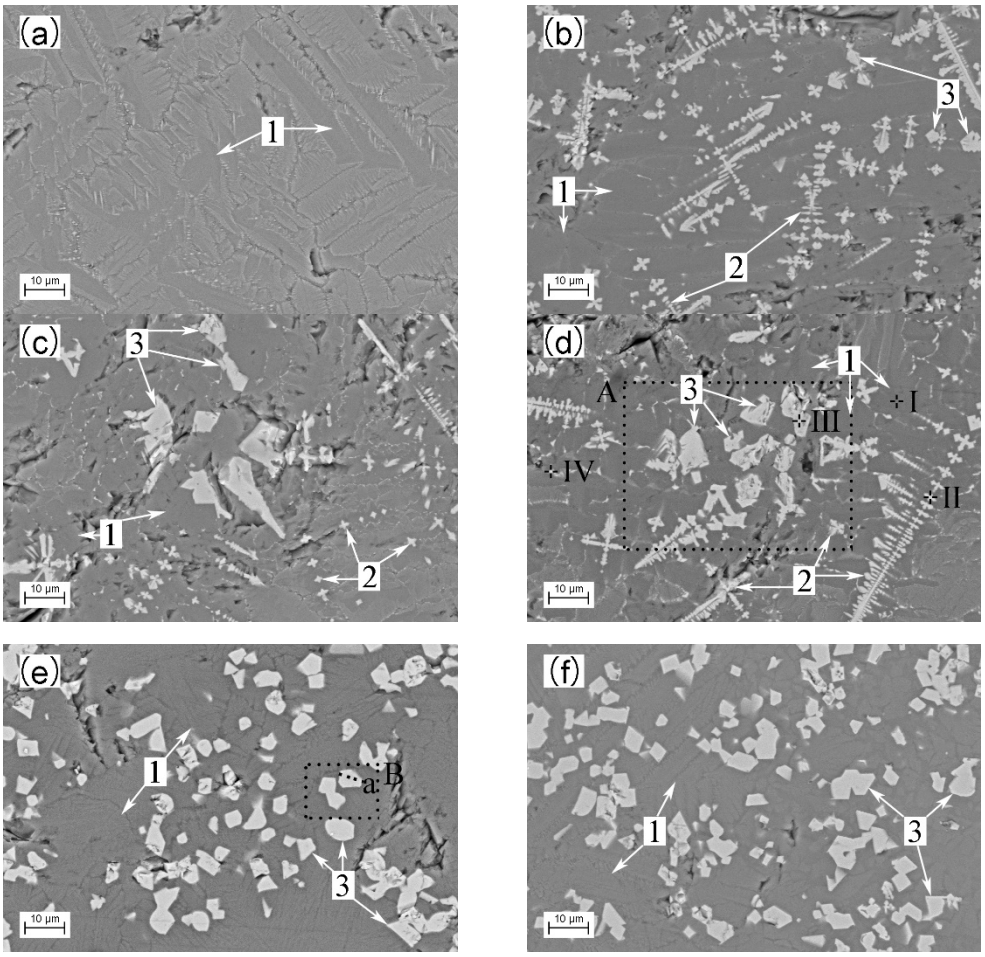

Figure 2. Effects of the Cr_2O_3 content of the microstructure of CaO-SiO_2-Fe_tO system. The numbers 1–3 in the figures represent the phases $CaFeSi_2O_6$, Fe_3O_4 and $Fe(Fe,Cr)_2O_4$, respectively. Samples A0 to A5 correspond to (**a**–**f**), respectively. The SEM mapping of area "A" in (**d**) is shown in Figure 3. The SEM mapping of area B and line "a" in (**e**) are shown in Figure 4. The EDS analysis results of points I, II, III, and IV in (**d**) are shown in Table 3.

Table 3. The EDS analysis results of each point in Figure 2d, at%.

No.	Fe	Cr	O	Si	Ca
I	7.0	—	64.5	19.4	9.1
II	25.5	—	64.4	7.0	3.1
III	25.1	12.4	62.5	—	—
IV	27.5	—	64.5	4.6	0.9

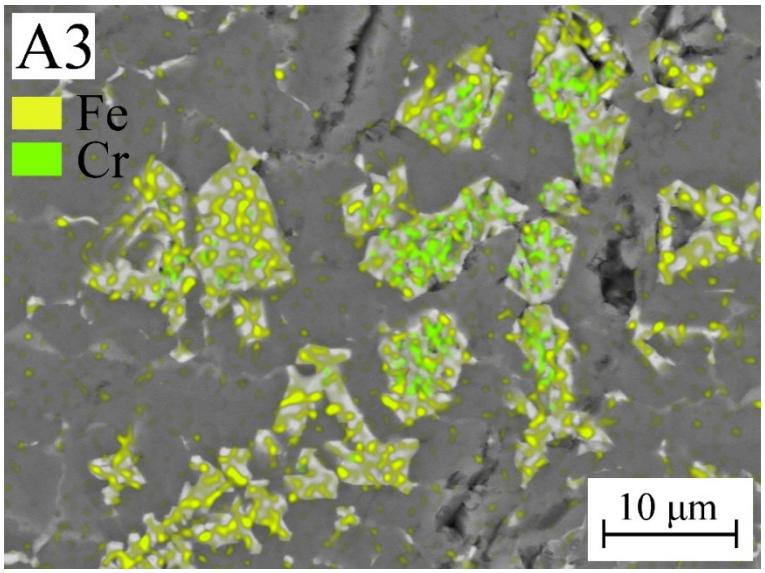

Figure 3. Distribution of Fe and Cr elements in the spine phase in Sample A3 according to EDS mapping results.

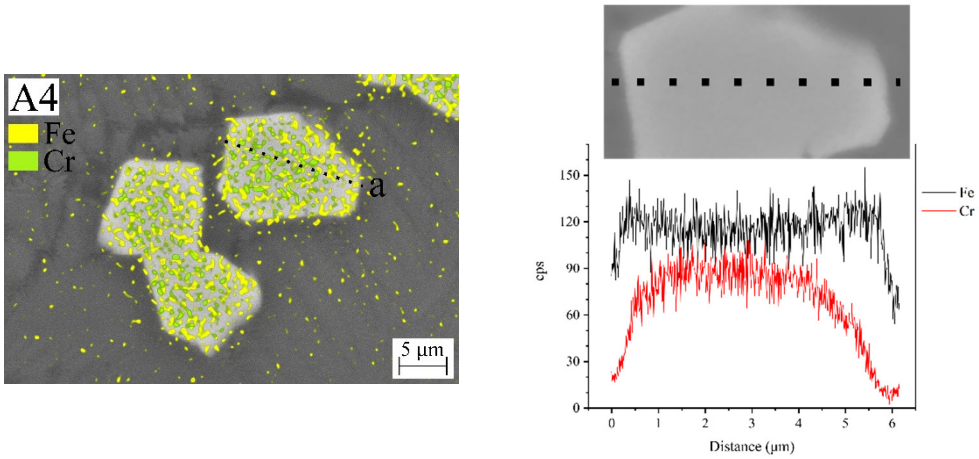

(**a**) (**b**)

Figure 4. Distribution of Fe and Cr elements in the spine phase in Sample A4 according to EDS mapping results. (**a**) Surface scanning result of area "A" in Figure 2d; (**b**) line scanning result of line "a" in Figure 2e.

There are two forms of spinel, dendritic spinel and granular spinel. As shown in Figure 3, the Fe element is enriched in both dendritic spinel crystals and granular spinel crystals, while Cr element is mostly concentrated in granular spinel crystals. Further, the concentration of Cr element decreases with increasing distance from the center of the granular spinel crystal, as shown in Figure 4. To sum up, the dendritic spinel phase is Fe_3O_4, and the granular spinel phase is an Fe_3O_4 layer wrapped around the core of $Fe(Fe,Cr)_2O_4$. Combined with the EDS composition analysis, the white phases in Figure 2b–d are dendritic Fe_3O_4 and granular $Fe(Fe,Cr)_2O_4$. The granular white phase in Figure 2e–f is granular $Fe(Fe,Cr)_2O_4$.

The average grain size of granular $Fe(Fe,Cr)_2O_4$ in Figure 2c–f was calculated by Image J software, and the results are shown in Figure 5. The grain size of the crystals is replaced by the diameter of a circle of the same area. With the increase of the Cr_2O_3 content, the number of $Fe(Fe,Cr)_2O_4$ crystals in the system increases and the average particle size decreases. In addition, the total area of the spinel phase in the 500× magnification SEM image of each sample was also counted. The area of the spinel phase has a positive linear correlation with

the Cr_2O_3 content, as shown in Figure 6. Therefore, the volume ratio of spinel phase in slag increases with the increase of Cr_2O_3 content.

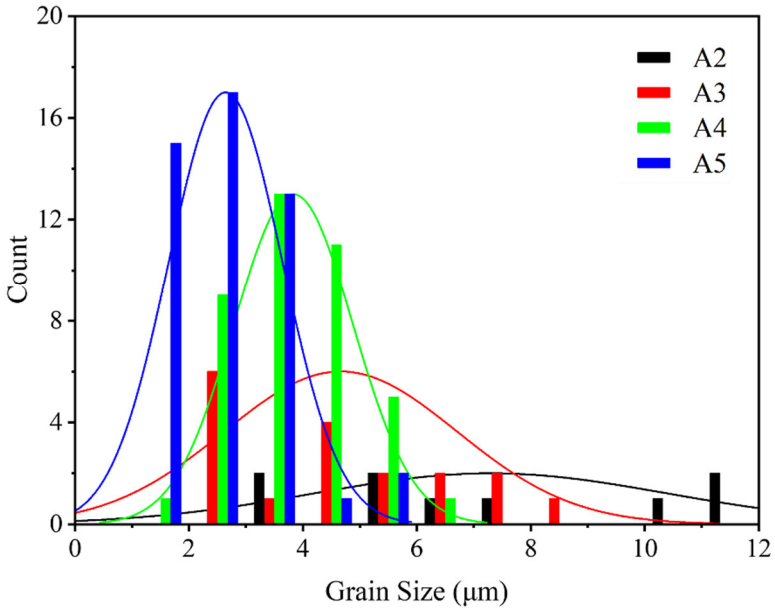

Figure 5. Relationship between Cr_2O_3 content and the average grain size of $Fe(Fe,Cr)_2O_4$ in Figure 2c–f.

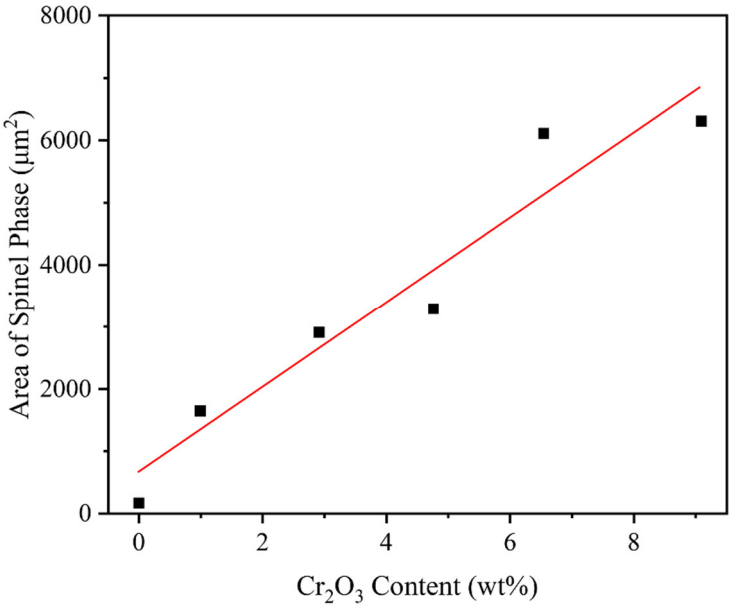

Figure 6. Relationship between Cr_2O_3 content and the amount of spinel at 1500 °C.

The elemental composition of the chain-like white particles in Figure 2a–d is shown in no. IV in Table 3. The authors believe that they are spinel particles precipitated in the late stage of slag solidification.

The composition of $Fe(Fe,Cr)_2O_4$ of each sample is shown in Table 4. As $w(Cr_2O_3)$ in the slag increased from 0.99 wt% to 9.09 wt%, the Fe element content in $Fe(Fe,Cr)_2O_4$ decreased from 36.9 at% to 22.1 at%, while the Cr element content increased from 1.1 at% to 14.9 at%. This shows that as Cr_2O_3 content increases, Fe^{3+} in the $FeO{\cdot}Fe_2O_3$ lattice is continuously replaced by Cr^{3+} to form $FeO{\cdot}Cr_2O_3$. The specific reaction equation is as follows:

$$(FeO{\cdot}Fe_2O_3) + (Cr_2O_3) = (FeO{\cdot}Cr_2O_3) + (Fe_2O_3) \quad (3)$$

Table 4. The EDS analysis results of phase 3 in Figure 2, at%.

No.	Fe	Cr	O	Si	Ca
A1	36.9	1.1	54.0	5.6	2.4
A2	29.9	7.0	61.7	1.0	0.4
A3	24.8	12.7	62.3	—	0.2
A4	25.4	13.8	60.4	0.2	0.2
A5	22.1	14.9	62.0	0.5	0.5

4. Discussion

4.1. Solidification Process of Cr_2O_3-Bearing CaO-SiO_2-Fe_tO Slags

FactSage 8.1 was used to calculate the solidification process of the 19% CaO-42% SiO_2-39% Fe_tO system with different Cr_2O_3 contents. The calculation used the Equilib module of FactSage 8.1, the database was set to FactPS and FToxide, the compound was set to pure solid, the solution phases were set to FToxid-SLAGA#1, FToxid-SPINA, FToxid-WOLLA, FToxid-OlivA#1, and FToxid -SLAGA#1 was used as the target phase. The species and quantity (g) were entered according to the proportions in Table 1, the solidification was set to start at a temperature of 1600 °C, the solidification step length to 1 °C, and the calculated stop temperature to be 1000 °C. The calculation results were exported in the form of pictures using the Figure module of FactSage 8.1, and the pictures were edited. We set the target temperature at 1500 °C and recorded the phase composition and mass (g) of the Spinel phase in the calculation results.

The influence of different content of Cr_2O_3 on the phase composition of the CaO-SiO_2-Fe_tO system during the solidification process is shown in Figure 7. The main phase of the system at the experimental temperature (1500 °C) is liquid slag and spinel. As the content of Cr_2O_3 added in the system increases, the content of spinel progressively increases, while the liquid phase gradually decreases. As shown in Figure 8, the content of the spinel phase of different samples were calculated by using FactSage 8.1. The spinel is mainly composed of $FeCr_2O_4$ and Fe_3O_4, and the $FeCr_2O_4$ is the main component, which accounts for more than 90 wt%. At 1500 °C, when the content of Cr_2O_3 increases from 0.99 to 9.09 wt%, the amount of spinel increases from 0.0799 wt% to 12.4722 wt%. Yu [15] studied the precipitation temperature, precipitation amount, and chemical composition of the chromium-containing spinel solid solution in the CaO-SiO_2-MgO-Cr_2O_3-FeO system, as well as the change law of the chromium element occurrence state. It was found that the spinel crystal is a high-temperature precipitation phase, the main components of which are $MgCr_2O_4$ and $FeCr_2O_4$. With the increase of FeO content, the precipitation temperature of chromium-bearing spinel gradually decreases, and its precipitation gradually increases. The increase of FeO content promoted the increase of the $FeCr_2O_4$ component in the spinel solid solution and inhibited the precipitation of $MgCr_2O_4$. Mou [16,17] found that the precipitation temperature of chromium-bearing spinel solid solution in the CaO-SiO_2-MgO-FeO-Cr_2O_3 system was more than 1700 °C, which can form a regular-shaped spinel solid solution in the slag. As shown in Equation (3), Cr_2O_3 combines with FeO in the slag to form $FeO{\cdot}Cr_2O_3$, which is precipitated under high temperature. At this time, the FeO existing in the slag can take $FeO{\cdot}Cr_2O_3$ as the matrix and participate in the precipitation of the spinel solid solution as the spinel crystal type, as shown in Equation (4).

$$x(Cr_2O_3) + (FeO) + (1-x)(Fe_2O_3) = Fe[xCr\cdot(1-x)Fe]_2O_4(s) \quad (4)$$

When the temperature is lower than 1100 °C, the liquid phase completely disappears. The main minerals in the system are calcium iron olivine ($CaFeSiO_4$), wollastonite ($CaFeSiO_4$), and spinel. With the increase of Cr_2O_3 in the system, the content of spinel increases significantly, the content of $CaSiO_3$ increases slightly, and the content of $CaFeSiO_4$ in the system decreases significantly. This phenomenon occurs because Cr_2O_3 easily reacts with FeO to form chromium-bearing spinel. As the content of chromium-bearing spinel increases, the content of FeO in the system is not enough to react with CaO to form $CaFeSiO_4$,

resulting in a decrease in the content of $CaFeSiO_4$. Moreover, excessive CaO and SiO_2 generate $CaFeSiO_4$, which increases the content of $CaFeSiO_4$.

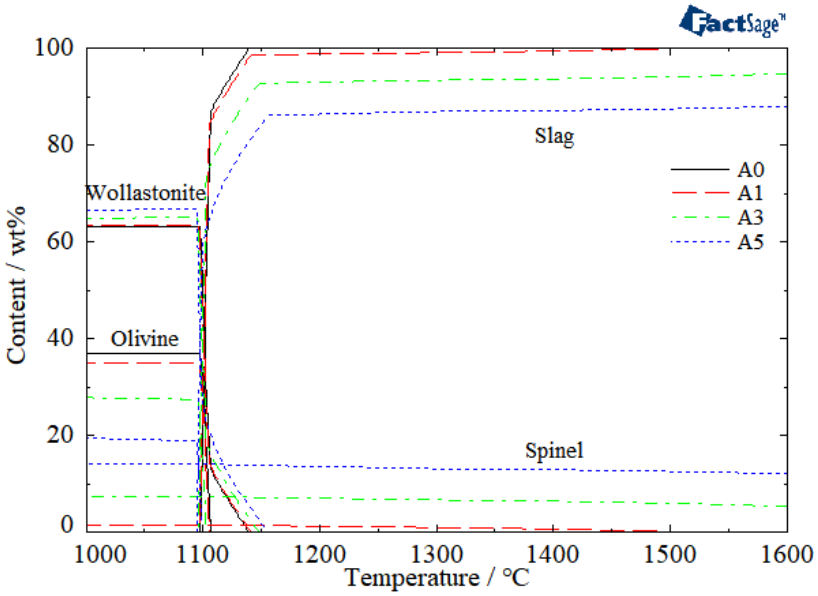

Figure 7. The solidification process of the CaO-SiO_2-Fe_tO-Cr_2O_3 system.

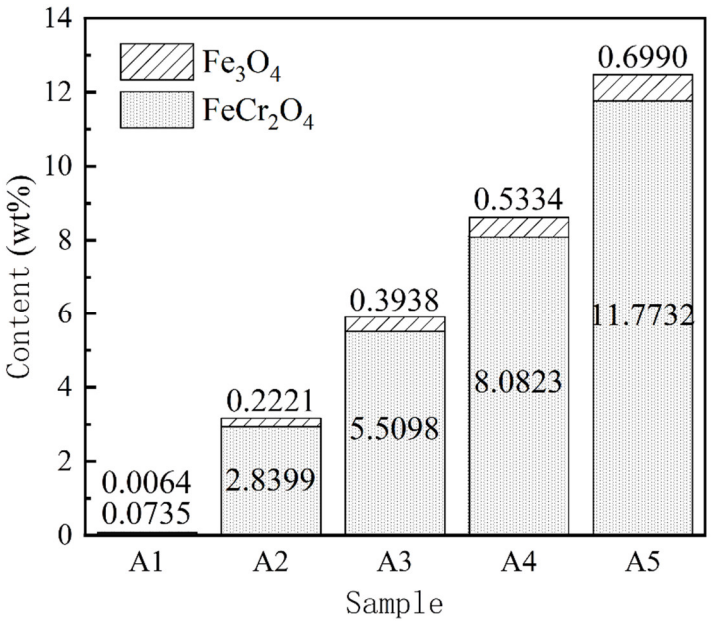

Figure 8. Relationship between Cr_2O_3 content and the components of spinel at 1500 °C.

It is well known that the crystallization process is divided into two stages, which is nucleation and growth. Nucleation in the melt can be divided into homogeneous nucleation and heterogeneous nucleation. That is, atoms or molecules in the melt spontaneously aggregate to form a new phase crystal nucleus or form a crystal nucleus on the surface of the solid phase particles suspended in the melt or mold wall. ΔT^* is used to denote the temperature at which the liquid phase can nucleate substantially. Among them, the degree of undercooling required for homogeneous nucleation is 0.2 T_m, and the degree of undercooling required for heterogeneous nucleation is only 0.02 T_m, where T_m is the melting point of the new phase. The melting point of $FeCr_2O_4$ (T_{m1}) is 2000 °C and the melting point of Fe_3O_4 (T_{m2}) is 1597 °C. If the difference between the melting point of the melt and

the test temperature (1500 °C) is simply regarded as the degree of undercooling (ΔT), then the degree of undercooling of $FeCr_2O_4$ is ΔT_1 = 2000 °C − 1500 °C = 0.22 T_{m1}. The degree of undercooling of Fe_3O_4 is ΔT_2 = 1597 °C − 1500 °C = 0.05 T_{m2}. Therefore, $FeCr_2O_4$ in the CaO-SiO_2-FetO system undergoes homogeneous nucleation at 1500 °C, while Fe_3O_4 undergoes heterogeneous nucleation on the surface of $FeCr_2O_4$. Zhang [18] studied the nucleation and growth kinetics of the spinel phase in 4.7% FeO-12.3% V_2O_3-18.4% SiO_2-12.5% TiO_2-8.2% MnO-4.1% MgO-2.8% CaO-3.4% Cr_2O_3-2.6% Al_2O_3 slag. The experimental results were similar to those in Figure 4. $FeCr_2O_4$ with the highest melting point was concentrated in the central part of the spinel crystal, while $FeTi_2O_4$ with the lowest melting point was concentrated in the outer part. FeV_2O_4 with a medium melting point had a relatively uniform distribution, but there was still a tendency for vanadium to concentrate in the central part of the spinel crystal.

As shown in Figure 9, when Cr_2O_3 is not added to the CaO-SiO_2-FetO system, the main phase of the slag is $CaFeSiO_6$, which has a melting point of 1150 °C. According to the thermodynamic analysis, there is no other solid phase material in the slag at this time. Fe_3O_4 undergoes heterogeneous nucleation, so a small number of small-sized dendrites are formed in the system. After 0.99 wt% to 4.76 wt% of Cr_2O_3 is added to the system, $FeCr_2O_4$ appears in the slag. $FeCr_2O_4$ nucleates and grows, and its shape is granular. With the progress of crystallization, the activity of Cr_2O_3 decreases, and the content of chromium in the chromium-bearing spinel gradually decreases. The nucleation and growth of Fe_3O_4 are carried out on the surface of $FeCr_2O_4$. Fe_3O_4 crystals precipitate in large quantities. As shown in Figure 9b, the center of the granular spinel is chromium-bearing spinel, while the edges are Fe_3O_4. When the content of Cr_2O_3 is further increased to 6.54 wt% and 9.09 wt%, all the spinel in the system is granular. Because of the high activity of Cr_2O_3 in the system, the nucleation rate of spinel crystals increases. A large number of granular spinel crystals are formed in the slag. The growth of a large number of crystal nuclei inhibits the crystal growth. The number of granular spinel crystals is positively correlated with the Cr_2O_3 content, but its particle size is negatively correlated with the Cr_2O_3 content. Furthermore, the thickness of the Fe_3O_4 layer around the granular spinel crystals is decreased by the sufficient Cr^{3+} in the system.

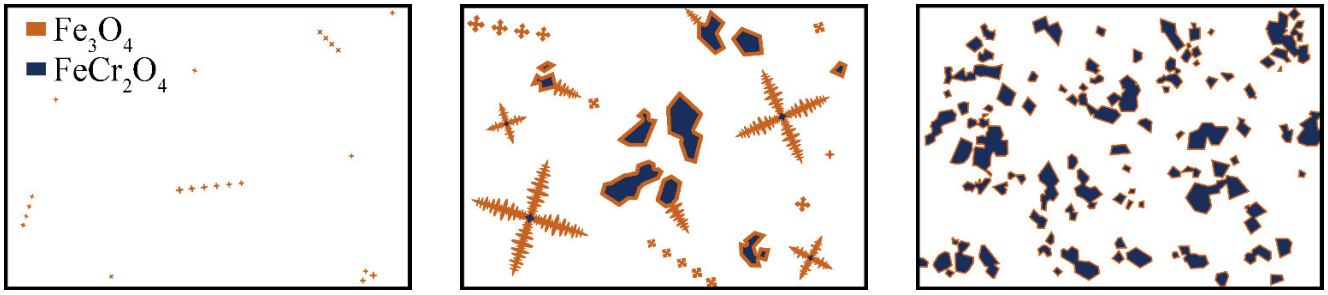

Figure 9. Crystallization mechanism of spinel in CaO-SiO_2-Fe_tO system at 1500 °C: (**a**) 0 wt% Cr_2O_3; (**b**) 0.99–4.76 wt% Cr_2O_3; (**c**) 6.54–9.09 wt% Cr_2O_3.

4.2. Effect of Different Cr_2O_3 Contents on the Viscosity of the Slag

In general, the Einstein–Roscoe equation was used to describe the relationship between the viscosity of liquid slag with solid particles (η_e) and the viscosity of fluids (η), as shown in Equation (5) [19,20].

$$\eta_e = \eta(1 - r\theta)^{-n} \quad (5)$$

where θ is the volume fraction of solid particles in liquid slag (%); r and n are empirical parameters, which are equal to 1.35 and 2.5, respectively.

With the addition of Cr_2O_3, a large number of solid particles in the CaO-SiO_2-Fe_tO system are suspended in the slag. It can be seen from the Equation (5) that this will increase the viscosity of the slag. In addition, Li et al. [4,21,22] believed that Cr^{3+} acted

as network former and increased the degree of polymerization (DOP) in Cr_2O_3-bearing CaO-SiO_2-MgO-Al_2O_3 slags. Hence, the addition of Cr_2O_3 to the slag increased the number of bridging oxygen atoms in the silicate structural units. Generally, the viscosity increased by increasing DOP.

The main task in the initial stage of the converter conversion is to quickly dissolve lime to achieve rapid slag formation, and quickly increase the basicity of the slag to increase the initial dephosphorization rate of the converter. Yan [23] studied the effect of Cr_2O_3 on the dissolution of lime in converter slag. It was found that the mass transfer in the boundary layer between slag and lime was the rate control step of lime dissolution. An increase of Cr_2O_3 and slag basicity delayed lime dissolution due to the formation of high-melting temperature phases of $FeO{\cdot}Cr_2O_3$ spinel and $2CaO{\cdot}SiO_2$ at the slag/lime reaction interface. The lime dissolution rate equation is shown in Equation (6) [24].

$$V_{CaO} = (D/\delta){\cdot}(C_s - C_b){\cdot}A \quad (6)$$

where V_{CaO} is the dissolution rate of CaO (mol/s); A is the surface area of lime (cm^2); D is the mass transfer coefficient of CaO (cm^2/s); δ is the thickness of the boundary layer (cm); and C_S and C_B are the saturated solubility of CaO in the slag and the actual concentration of CaO in the slag (mol/cm^3).

It can be seen from Equation (6) that the increase of viscosity of the slag leads to a decrease in the mass transfer coefficient of lime and an increase in the thickness of the boundary layer. Therefore, the increase of the Cr_2O_3 content in the CaO-SiO_2-FetO system will not be conducive to the dissolution of lime in the initial stage of the converter. In addition, with the increase of $w(Cr_2O_3)$, Cr_2O_3 reacts with FeO to form high-melting chromium-bearing spinel, and the melting temperature of the slag gradually rises. When $w(Cr_2O_3)$ in the slag is 6.54 wt%, the melting temperature of the slag (1335 °C) is higher than the temperature of semi-steel into the converter (about 1280 °C to 1310 °C) [25], which will cause difficulty for the slag formation at the initial stage of the converter. Therefore, as the content of Cr_2O_3 increases from 0 wt% to 9.09 wt% in the system, the melting temperature and viscosity of the slag show an upward trend, which is unfavorable for converter production.

5. Conclusions

In this article, Factsage8.1, X-ray diffraction (XRD), scanning electron microscope (SEM-EDS) and a high-temperature melting point tester were used to study the influence of Cr_2O_3 on the physical and chemical properties of the CaO-SiO_2-FetO system at 1500 °C. The main conclusions are summarized as follows:

1. In the CaO-SiO_2-FetO system, when the temperature was 1500 °C, the basic liquid phase of the system was $CaFeSi_2O_6$. As the Cr_2O_3 content in the system increased from 0 wt% to 4.76 wt%, dendritic Fe_3O_4 and granular chromium-containing iron spinel ($Fe(Fe,Cr)_2O_4$) formed in the slag. With the content of Cr_2O_3 further increased to 9.09 wt%, the spinel phase was completely transformed to the chromium-containing iron spinel phase.
2. With the increase of $w(Cr_2O_3)$ in the CaO-SiO_2-FetO system from 0 wt% to 9.09 wt%, the melting temperature of the slag increased from 1223 °C to 1354 °C.
3. The content of the spinel phase in the CaO-SiO_2-Fe_tO system gradually increased with the increase of $w(Cr_2O_3)$ from 0 wt% to 9.09 wt%, while the content of the liquid phase decreased. The viscosity of the slag therefore increased. This had an adverse effect on the formation of slag and the rapid dissolution of lime at the initial stage of the converter.

Author Contributions: Conceptualization, J.L.; methodology, J.L. and S.L.; software, J.L. and S.L.; validation, Y.Y. and H.Z.; formal analysis, S.L.; investigation, S.L. and Y.Y.; resources, Y.Y.; data curation, S.L.; writing—original draft preparation, S.L.; writing—review and editing, J.L. and H.Z.; visualization, S.L., J.L. and H.Z.; supervision, J.L.; project administration, Y.Y.; funding acquisition, J.L., Y.Y. and H.Z. All authors have read and agreed to the published version of the manuscript.

Funding: This work was financially supported by the National Natural Science Foundation of China (no. 52074197, no. 51974210), Hubei Provincial Natural Science Foundation (no. 2019CFB697), and State Key Laboratory of Refractories and Metallurgy, Wuhan University of Science and Technology.

Institutional Review Board Statement: Not applicable.

Informed Consent Statement: Not applicable.

Data Availability Statement: Not applicable.

Conflicts of Interest: The authors declare no conflict of interest.

References

1. Zhao, L.; Wang, L.; Qi, T.; Chen, D.; Zhao, H.; Liu, Y. A novel method to extract iron, titanium, vanadium, and chromium from high-chromium vanadium-bearing titanomagnetite concentrates. *Hydrometallurgy* **2014**, *149*, 106–109. [CrossRef]
2. Tang, J.; Chu, M.; Feng, C.; Li, F.; Tang, Y.; Liu, Z. Coupled Effect of Valuable Components in High-Chromium Vanadium-bearing Titanomagnetite during Oxidization Roasting. *ISIJ Int.* **2016**, *56*, 1342–1351. [CrossRef]
3. Li, W.; Fu, G.Q.; Chu, M.S.; Zhu, M.Y. Oxidation induration process and kinetics of Hongge vanadium titanium-bearing magnetite pellets. *Ironmak. Steelmak.* **2016**, *44*, 294–303. [CrossRef]
4. Chen, M.; Deng, H.; Wang, N.; Zhang, G. Limestone Dissolution in Converter Slag: Kinetics and Influence of Decomposition Reaction. *ISIJ Int.* **2018**, *58*, 2271–2279. [CrossRef]
5. Babenko, A.A.; Shartdinov, R.R.; Upolovnikova, A.G.; Smetannikov, A.N.; Mikhailova, L.Y. Effect of basicity and chromium oxide on the viscosity of boron-containing slags. *IOP Conf. Ser. Mater. Sci. Eng.* **2020**, *966*, 012012. [CrossRef]
6. Huang, W.; Liu, Y. Crystallization Behavior and Growth Mechanisms of Spinel Crystals in Vanadium-Containing Slags. *ISIJ Int.* **2020**, *60*, 2183–2190. [CrossRef]
7. Cheng, G.; Xue, X.; Gao, Z.; Jiang, T.; Yang, H.; Duan, P. Effect of Cr_2O_3 on the Reduction and Smelting Mechanism of High-Chromium Vanadium-Titanium Magnetite Pellets. *ISIJ Int.* **2016**, *56*, 1938–1947. [CrossRef]
8. Qiu, G.; Chen, L.; Zhu, J.; Lv, X.; Bai, C. Effect of Cr_2O_3 Addition on Viscosity and Structure of Ti-bearing Blast Furnace Slag. *ISIJ Int.* **2015**, *55*, 1367–1376. [CrossRef]
9. Xu, C.; Wang, W.; Zhou, L.; Xie, S.; Zhang, C. The Effects of Cr_2O_3 on the Melting, Viscosity, Heat Transfer, and Crystallization Behaviors of Mold Flux Used for the Casting of Cr-Bearing Alloy Steels. *Metall. Mater. Trans. B* **2014**, *46*, 882–892. [CrossRef]
10. Li, Q.; Gao, J.; Zhang, Y.; An, Z.; Guo, Z. Viscosity Measurement and Structure Analysis of Cr_2O_3-Bearing CaO-SiO_2-MgO-Al_2O_3 Slags. *Metall. Mater. Trans. B* **2016**, *48*, 346–356. [CrossRef]
11. Wu, T.; Zhang, Y.; Yuan, F.; An, Z. Effects of the Cr_2O_3 Content on the Viscosity of CaO-SiO_2-10 Pct Al_2O_3-Cr_2O_3 Quaternary Slag. *Metall. Mater. Trans. B* **2018**, *49*, 1719–1731. [CrossRef]
12. Xu, R.Z.; Zhang, J.L.; Wang, Z.Y.; Jiao, K.X. Influence of Cr_2O_3 and B_2O_3 on Viscosity and Structure of High Alumina Slag. *Steel Res. Int.* **2017**, *88*, 1600241. [CrossRef]
13. Liu, Z.; Dekkers, R.; Blanpain, B.; Guo, M. Experimental Study on the Viscosity of Stainless Steelmaking Slags. *ISIJ Int.* **2019**, *59*, 404–411. [CrossRef]
14. Chen, K.; Zheng, Z.; Gao, X. A Novel Process Control Model for Extracting Vanadium Semi-Steel in Basic Oxygen Furnace Based on Steelmaking Mechanism. *Steel Res. Int.* **2012**, *83*, 456–464. [CrossRef]
15. Yu, Y.; Wang, D.; Li, J.L.; Zhu, H.Y.; Xue, Z.L. Thermodynamic calculation of FeO effect on precipitation of spinel containing chromium in CaO-SiO_2-MgO-Al_2O_3-Cr_2O_3 system. *J. Wuhan Univ. Sci. Technol. Nat. Sci. Ed.* **2018**, *41*, 15–19. [CrossRef]
16. Mou, Q.Q.; Li, J.L.; Zeng, Q.; Zhu, H.Y. Effect of Fe_2O_3 on the size and components of spinel crystals in the CaO-SiO_2-MgO-Al_2O_3-Cr_2O_3 system. *Int. J. Miner. Metall. Mater.* **2019**, *26*, 1113–1119. [CrossRef]
17. Zeng, Q.; Li, J.; Mou, Q.; Zhu, H.; Xue, Z. Effect of FeO on Spinel Crystallization and Chromium Stability in Stainless Steel-Making Slag. *JOM* **2019**, *71*, 2331–2337. [CrossRef]
18. Zhang, X.; Xie, B.; Diao, J.; Li, X.J. Nucleation and growth kinetics of spinel crystals in vanadium slag. *Ironmak. Steelmak.* **2013**, *39*, 147–154. [CrossRef]
19. Yuan, F.; Zhao, Z.; Zhang, Y.-l.; Wu, T. Influence of Cr_2O_3 content on viscosity and rheological behavior of Cr_2O_3-containing slags. *J. Iron Steel Res. Int.* **2021**, *29*, 601–611. [CrossRef]
20. Zhang, G.-H.; Zhen, Y.-L.; Chou, K.-C. Influence of TiC on the Viscosity of CaO–MgO–Al_2O_3–SiO_2–TiC Suspension System. *ISIJ Int.* **2015**, *55*, 922–927. [CrossRef]
21. Huang, W.J.; Zhao, Y.H.; Yu, S.; Zhang, L.X.; Ye, Z.C.; Wang, N.; Chen, M. Viscosity Property and Structure Analysis of FeO-SiO_2-V_2O_3-TiO_2-Cr_2O_3 Slags. *ISIJ Int.* **2016**, *56*, 594–601. [CrossRef]

22. Hou, X.; Xiao, G.; Ding, D.; Zhang, N.; Gao, Y. Effects of Cr_2O_3 content on viscosity and microstructure of copper converter slag. *J. Non-Cryst. Solids* **2021**, *574*, 121147. [CrossRef]
23. Yan, W.; Chen, W.; Zhao, X.; Yang, Y.; McLean, A. Effect of Cr_2O_3 Pickup on Dissolution of Lime in Converter Slag. *High Temp. Mater. Processes* **2017**, *36*, 937–946. [CrossRef]
24. Madhurai, M.; Gupta, P.; Koopmans, P.; Overbosch, A.; Boom, R.; Deo, B. Theoretical and Practical Aspects of Dissolution of Lime in Laboratory Experiments and in BOF. On-line dynamic control of steelmaking processes, including chaotic dyanamical systems. In Proceedings of the 5th European Oxygen Steelmaking Conference, Aachen, Germany, 26–28 June 2006. [CrossRef]
25. Yuan, Z.F.; Zhou, J.C.; Liao, D.H.; Huang, W.L.; Mukai, K. Carburization and desulphurisation of the semi-steel during plasma heating. *Steel Res.* **2002**, *73*, 175–179. [CrossRef]